

Effective scan parameter setting of Quiet Suite combined readout segmented multi-shot EPI DWI (qRESOLVE) for decrease of image distortion and acoustic noise with a 3T MRI scanner

Quiet Suite 併用 readout segmented multi shot EPI DWI (qRESOLVE) による画像歪みおよび撮像音低減を目的としたパラメーターについての検討

KOBAYASHI Yoshikazu¹⁾, KANDA Toshimitsu²⁾, SAITO Yoko³⁾,

1) ShinSapporo neurosurgical hospital / Hirosaki University Graduate School of Health Sciences, Radiologic technologist

2) ShinSapporo neurosurgical hospital, Radiologic technologist

3) Department of Radiation Science, Hirosaki University Graduate School of Health Sciences, professor, Medical doctor

Key words: Quiet Suite combined readout segmented multi shot EPI DWI (qRESOLVE), image distortion, acoustic noise, echo spacing, parallel imaging factor

【Abstract】

The purpose of this study was to determine effective scan parameter settings for decreasing image distortion and acoustic noise by scanning phantoms with various parameters using the Quiet Suite combined readout segmented multi-shot echo planar imaging (qRESOLVE) with a 3T MRI scanner. The distortion rate of the slit area in the phantom was calculated in the phantom experiment. Furthermore, peak sound pressure levels were calculated. The results showed that with a decrease in echo spacing (ES) and field of view (FOV), for a thin slice thickness, an increase in the parallel imaging factor (PIF) and matrix size (MS) were effective for decreasing image distortion ($p < 0.017$). To decrease acoustic noise, an increase in ES, number of segments (SEG), repetition time (TR), and FOV, and a decrease in PIF and MS, were effective ($p < 0.017$). With respect to routine clinical examinations, a decrease in ES and an increase in PIF were effective for decreasing image distortion, and with an increase in ES, a decrease in PIF and SEG were effective for decreasing acoustic noise.

【要旨】

研究目的は、Quiet Suite併用readout segmented multi-shot EPI DWI (qRESOLVE) で、各種パラメーターを変更させファントムを撮像し、画像歪みおよび撮像音低減に効果的なパラメーターを決定することである。実験で歪み率を算出し、撮像音を測定しピーク音圧レベルを算出した。結果、画像歪み低減には、エコースペース (ES)・FOV・slice厚を小さく、パラレルイメージング係数 (PIF)・マトリクスサイズ (MS) を大きくすることが有効であった。撮像音低減には、ES・セグメント数 (SEG)・TR・FOVを大きく、PIF・MSを小さくすることが有効であった。

Introduction

Diffusion-weighted imaging (DWI) using single-shot echo planar imaging (EPI) is useful for the diagnosis of acute cerebral infarction and brain tumors. However, it has the disadvantages of causing significant image distortion and very loud acoustic noise¹⁾. Image distortion may degrade the diagnostic accuracy, and loud acoustic noise causes

discomfort and anxiety in patients. Moreover, a decrease in acoustic noise is important to avoid hearing impairment. Siemens Healthineers has developed readout segmented multi-shot EPI DWI (RESOLVE : readout segmentation of long variable echo-trains) as an imaging method to improve image distortion. RESOLVE is a new multi-shot EPI DWI that segments the readout direction in k-space. RESOLVE decreases the readout time in k-space, which allows short echo spacing, and can be used in conjunction with parallel imaging methods. In addition, parallel imaging methods can be used to decrease dephasing and image distortion²⁾. However, RESOLVE has the disadvantages of loud acoustic noise resulting from the fast switching of the gradient field

小林 由和¹⁾, 神田 俊光²⁾, 齋藤 陽子³⁾

1) 新さっぽろ脳神経外科病院放射線部／弘前大学大学院保健学研究科, 診療放射線技師

2) 新さっぽろ脳神経外科病院放射線部, 診療放射線技師

3) 弘前大学大学院保健学研究科, 教授, 医師

Received June 17, 2022; accepted January 6, 2023

and short echo spacing. Recently, RESOLVE with the Quiet Suite method (qRESOLVE) was developed to decrease discomfort and avoid hearing impairment during routine clinical examination. qRESOLVE is an effective sequence that achieves silence by automatically optimizing the shape of the gradient field (the angle of the gradient field is decreased)^{3,4)}. In this study, a phantom was scanned with various qRESOLVE parameters, and effective parameter settings for decreasing image distortion and acoustic noise were investigated.

Materials and Methods

1. Equipment

An MR scanner (MAGNETOM Skyra syngo VE11 3.0T (Siemens Healthineers)) was used. The coil was a 20 channels head/neck coil (Siemens Healthineers). A spherical phantom (Siemens Healthineers : D165{1.25gNaSO₄ × 6H₂O}) and Japanese Industrial Standards (JIS) phantom (Nikko Finds Industries : 95-1108Z type) were used.

2. Scan parameters

In qRESOLVE, the echo spacing (ES), parallel imaging factor (PIF), number of segments (SEG), phase partial fourier (PpF), repetition time (TR), matrix size (MS), slice thickness (ST), and field of view (FOV) were varied. The scan parameters are listed in Tables 1-1 through 1-8. The center of the phantom was set to the isocenter, and the scan plane was a transverse section. The phase encoding direction was set to the left-right direction, motion probing gradient (MPG) pulses were applied in three axes, and a monopolar three-scan trace was used in diffusion mode. The parallel imaging method used was generalized auto-calibrating partially parallel acquisitions (GRAPPA)⁵⁾.

3. Examination of distortion rate

The distortion rate is generally calculated using the area method⁶⁾. However, in this study, ST, MS, and FOV also varied, and the image could not be subtracted. Therefore, the distortion rate was defined as in Eq. (1), based on a report by Kajisako et al.⁷⁾ qRESOLVE with various scan parameters (Tables 1-1 through 1-8) were evaluated in comparison with T₂-weighted images (T₂WI) (Table 2). The slit area in the JIS phantom was imaged for both sequences. Scans were performed 10 times to decrease sampling error, and the average value was calculated.

$$\text{Distortion rate} = (W_q/W_t) \times 100 \dots\dots\dots(1)$$

where W_q is the slit width measured by qRESOLVE and W_t is the slit width measured by T₂WI. As shown in Fig.1, W_t and W_q were measured by drawing a straight line perpendicular to the slits at both ends. The closer the distortion rate is to 100, the less image distortion is present.

4. Examination of acoustic noise

4.1. Peak sound pressure level

A spherical phantom was scanned using qRESOLVE (Tables 1-1 through 1-8) with various scan parameters to measure acoustic noise. The measurement position of acoustic noise (●) is shown in Fig.2. The measurement time was set to 1 min (because the scan time for DWI using single-shot echo planar imaging used in routine clinical examination is approximately 1 min). The maximum value during the measurement period was used as the peak sound pressure level (L_{peak}) (dB). Scans were performed 10 times to decrease sampling error, and the average value was calculated. An acoustic sound measurement system (Kenneth Inc. : YC-30) was used. The settings of the acoustic noise measurement system are as follows : the frequency-weighting characteristic was

Table 1-1 Imaging parameters of qRESOLVE with various ES values

ES(ms)	0.5	0.6	0.7	0.78	0.94	1
TR(ms)			4500			
TE(ms)	83	92	100	107	122	127
Band width(Hz/pixel)	620	465	372	318	250	228
FOV(mm)			220×220			
Slice thickness(mm)			5			
Slice gap(%)			20			
MS			192×192			
number of excitations			1			
SEG			7			
PIF			GRAPPA 2			
PpF			Off			
Fat suppression			CHESS			
b-factor(s/mm ²)			0, 1000			
Reacquisition mode			on			
Filter	Raw filter, Distortion Correction(2D), Prescin Normalize					

Table 1-4 Imaging parameters of qRESOLVE with various PpF values

PpF	Off	7/8	6/8
TR(ms)		4500	
TE(ms)	122	101	81
Band width(Hz/pixel)		250	
FOV(mm)		220×220	
Slice thickness(mm)		5	
Slice gap(%)		20	
MS		192×192	
number of excitations		1	
PIF		GRAPPA 2	
SEG		7	
ES(ms)		0.94	
Fat suppression		CHESS	
b-factor(s/mm ²)		0, 1000	
Reacquisition mode		on	
Filter	Raw filter, Distortion Correction(2D), Prescin Normalize		

Table 1-2 Imaging parameters of qRESOLVE with various PIF values

PIF	2	3	4
TR(ms)		4500	
TE(ms)	122	94	81
Band width(Hz/pixel)	250	260	277
FOV(mm)		220×220	
Slice thickness(mm)		5	
Slice gap(%)		20	
MS		192×192	
number of excitations		1	
SEG		7	
ES(ms)		0.94	
PpF		Off	
Fat suppression		CHESS	
b-factor(s/mm ²)		0, 1000	
Reacquisition mode		on	
Filter	Raw filter, Distortion Correction(2D), Prescin Normalize		

Table 1-5 Imaging parameters of qRESOLVE with various MS values

MS	128×128	160×160	192×192	226×226
TR(ms)		4500		
TE(ms)	94	108	122	137
Band width(Hz/pixel)	275	256	250	240
FOV(mm)		220×220		
Slice thickness(mm)		5		
Slice gap(%)		20		
number of excitations		1		
SEG		7		
PIF		GRAPPA 2		
ES(ms)		0.94		
PpF		Off		
Fat suppression		CHESS		
b-factor(s/mm ²)		0, 1000		
Reacquisition mode		on		
Filter	Raw filter, Distortion Correction(2D), Prescin Normalize			

Table 1-3 Imaging parameters of qRESOLVE with various SEG values

SEG	3	5	7	9	11
TR(ms)			4500		
TE(ms)	122	122	122	122	122
Band width(Hz/pixel)	521	326	250	207	176
FOV(mm)			220×220		
Slice thickness(mm)			5		
Slice gap(%)			20		
MS			192×192		
number of excitations			1		
PIF			GRAPPA 2		
ES(ms)			0.94		
PpF			Off		
Fat suppression			CHESS		
b-factor(s/mm ²)			0, 1000		
Reacquisition mode			on		
Filter	Raw filter, Distortion Correction(2D), Prescin Normalize				

Table 1-6 Imaging parameters of qRESOLVE with various TR values

TR(ms)	4030	4500	5000	5500	6000
TE(ms)			122		
Band width(Hz/pixel)			250		
FOV(mm)			220×220		
Slice thickness(mm)			5		
Slice gap(%)			20		
MS			192×192		
number of excitations			1		
SEG			7		
PIF			GRAPPA 2		
ES(ms)			0.94		
PpF			Off		
Fat suppression			CHESS		
b-factor(s/mm ²)			0, 1000		
Reacquisition mode			on		
Filter	Raw filter, Distortion Correction(2D), Prescin Normalize				

Table 1-7 Imaging parameters of qRESOLVE with various FOV values

FOV(mm)	100×100	150×150	200×200	250×250	300×300
TR(ms)			4500		
TE(ms)			122		
Band width(Hz/pixel)	277	260	250	241	237
Slice thickness(mm)			5		
Slice gap(%)			20		
MS			192×192		
number of excitations			1		
SEG			7		
PIF			GRAPPA 2		
ES(ms)			0.94		
PpF			Off		
Fat suppression			CHESS		
b-factor(s/mm ²)			0, 1000		
Reacquisition mode			on		
Filter	Raw filter, Distortion Correction(2D), Prescin Normalize				

Table 1-8 Imaging parameters of qRESOLVE with various ST values

ST(mm)	1	3	5	7	10
TR(ms)			4500		
TE(ms)			122		
Band width(Hz/pixel)			250		
FOV(mm)			220×220		
Slice gap(%)			20		
MS			192×192		
number of excitations			1		
SEG			7		
PIF			GRAPPA 2		
ES(ms)			0.94		
PpF			Off		
Fat suppression			CHESS		
b-factor(s/mm ²)			0, 1000		
Reacquisition mode			on		
Filter	Raw filter, Distortion Correction(2D), Prescin Normalize				

Table 2 Imaging parameters of T₂WI

	T ₂ WI
TR(ms)	4500
TE(ms)	88
Band width(Hz/pixel)	193
FOV(mm)	220×220
Slice gap(%)	20
MS	192×192
Slice thickness(mm)	5
number of excitations	1
PIF	no used
ES(ms)	9.8
Filter	Distortion Correction(2D), Prescin Normalize

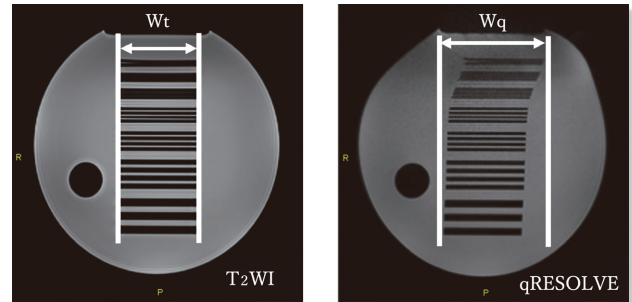


Fig.1 Slit width measuring method

Straight lines were drawn at the slits on both ends ; W_t was measured on T₂WI, and W_q was measured using qRESOLVE.

set to C, and the time-weighting characteristic was set to Fast. Furthermore, we calculated the sound pressure level (dB) between the maximum and minimum of L_{peak} using various parameters and Eq. (2)⁸⁾ :

$$\text{Sound pressure level (dB)} = 20\log_{10}(A/A_0) \dots\dots\dots(2)$$

where A is the observed value and A₀ is the reference value (20 × 10⁻⁵ [Pa]).

4.2. Time waveform analysis

The spherical phantom was scanned by qRESOLVE with various scan parameters (Tables 1-1 through 1-8) to analyze the time waveform of acoustic noise. The recording

position of acoustic noise (●) is shown in Fig.2. The recorded data was transferred to a personal computer (Microsoft Surface Pro3), and the time waveform was analyzed. A recording device for acoustic noise (TASCAM Inc. : DR-05X) was used. Frequency analysis software (NCH software Inc. : WavePad audio editing software) was used.

5. Statistical analysis

The distortion rate and acoustic noise (L_{peak}) obtained from the phantom experiment were evaluated to determine significant differences using the Friedman test. The significance level was corrected using the Bonferroni method for multiple comparisons. EZR⁹⁾ was used for statistical analysis.

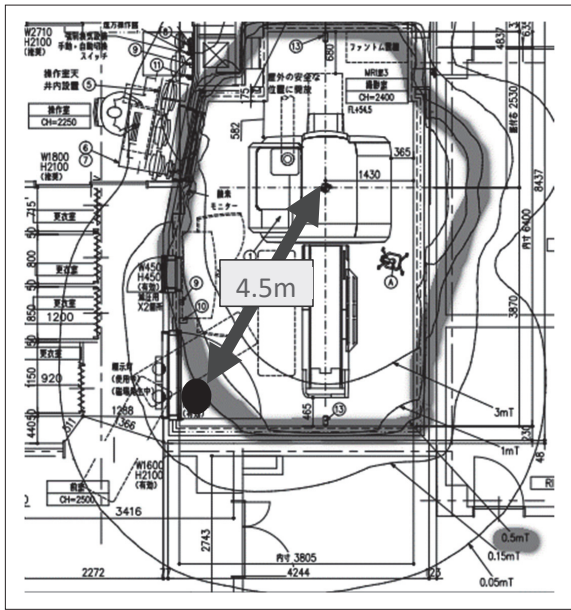


Fig.2 Acoustic noise and time waveform measurement position

The black dot (●) shows the measurement position for acoustic noise and time waveform analysis. The distance from the center of the gantry was approximately 4.5 m and was located outside the five Gaussian lines (gray lines). The height of the measurement point was 1.3 m above the ground.

Results

1. Examination of distortion rate

1-1. Distortion rate with various ES values

The distortion rates with various ES values are listed in Table 3-1. The distortion rate increased with an increase in ES. There was a significant difference between ES values ($p < 0.003$).

1-2. Distortion rate with various PIF values

The distortion rates with various PIF values are listed in Table 3-2. The distortion rate decreased with an increase in PIF. There was a significant difference between PIF values ($p < 0.017$).

1-3. Distortion rate with various SEG values

The distortion rates with various SEG values are listed in Table 3-3. There was no change in the distortion rate with an increase in SEG. No significant difference was observed

Table 3-1 Distortion rate with various ES values

ES(ms)	0.5	0.6	0.7	0.78	0.94	1
distortion rate(%)	115.8	118.3	121.3	123.4	128.2	130.6

Table 3-2 Distortion rate with various PIF values

PIF	2	3	4
distortion rate(%)	121	114.1	111.2

Table 3-3 Distortion rate with various SEG values

SEG	3	5	7	9	11
distortion rate(%)	119.2	119.2	119.2	119.3	119.3

Table 3-4 Distortion rate with various PpF values

PpF	Off	7/8	6/8
distortion rate(%)	120.9	121.5	123.6

Table 3-5 Distortion rate with various TR values

TR(ms)	4030	4500	5000	5500	6000
distortion rate(%)	120.9	120.9	120.9	120.8	120.9

Table 3-6 Distortion rate with various MS values

MS	128×128	160×160	192×192	226×226
distortion rate(%)	119.4	118.3	117.6	117.2

Table 3-7 Distortion rate with various ST values

ST(mm)	1	3	5	7	10
distortion rate(%)	113	114.4	118.4	120.2	123

Table 3-8 Distortion rate with various FOV values

FOV(mm)	100×100	150×150	200×200	250×250	300×300
distortion rate(%)	not measured	113.6	118.4	123.5	128.7

between any of the SEG values ($p > 0.005$).

1-4. Distortion rate with various PpF values

The distortion rates with various PpF values are shown in Table 3-4. The distortion rate decreased with a decrease in PpF. There was a significant difference between any PpF values ($p < 0.017$).

1-5. Distortion rate with various TR values

The distortion rates with various TR values are shown in Table 3-5. No significant difference was observed between the TR values ($p > 0.005$). TR did not affect the distortion rate.

1-6. Distortion rate with various MS values

The distortion rates with various MS values are shown in Table 3-6. The distortion rate decreased with an increase in MS. There was a significant difference between MS values ($p < 0.013$).

1-7. Distortion rate with various ST values

The distortion rates with various ST values are listed in Table 3-7. The distortion rate increased with increasing ST. There was a significant difference between ST values ($p < 0.005$).

1-8. Distortion rate with various FOV values

The distortion rates with various FOV values are listed in Table 3-8. The distortion rate increased with an increase in the FOV. There was a significant difference between FOV values ($p < 0.013$).

2. Examination of acoustic noise

2-1. Examination of L_{peak}

2-1-1. L_{peak} with various ES values

The results for L_{peak} with various ES values are shown in Table 4-1. With an increase in ES, L_{peak} decreased to 0.94 ms. There was a significant difference between all ES values except between 0.7 and 0.78 ms ($p < 0.003$). Using this result, the phantom experiment was set to 0.94 ms (minimum value of L_{peak}). There was a level difference of 14.1 dB between the maximum (with an ES of 0.5 ms) and minimum (with an ES of 0.94 ms). According to Eq.(2), the sound pressure level with an ES of 0.5 ms was 5.1 times higher than that with an ES of 0.94 ms.

2-1-2. L_{peak} with various PIF values

The results for L_{peak} with various PIF values are listed in Table 4-2. L_{peak} increased with increasing PIF. There was a significant difference between PIF values ($p < 0.017$). There was a level difference of 1.6 dB between the maximum (with a PIF of 4) and

Table 4-1 L_{peak} with various ES values

ES(ms)	0.5	0.6	0.7	0.78	0.94	1
L_{peak} (dB)	94.8	87.7	86.6	86.8	80.7	81.7

Table 4-2 L_{peak} with various PIF values

PIF	2	3	4
L_{peak} (dB)	82.2	83.2	83.8

Table 4-3 L_{peak} with various SEG values

SEG	3	5	7	9	11
L_{peak} (dB)	86.3	83.4	82.6	81.9	81.6

Table 4-4 L_{peak} with various PpF values

PpF	Off	7/8	6/8
L_{peak} (dB)	82.4	82.3	82.5

Table 4-5 L_{peak} with various TR values

TR(ms)	4030	4500	5000	5500	6000
L_{peak} (dB)	82.9	82.7	82.4	82.3	82.2

Table 4-6 L_{peak} with various MS values

MS	128×128	160×160	192×192	226×226
L_{peak} (dB)	82.1	82.1	82.8	82.5

Table 4-7 L_{peak} with various ST values

ST(mm)	1	3	5	7	10
L_{peak} (dB)	83	82.9	82.8	82.8	82.8

Table 4-8 L_{peak} with various FOV values

FOV(mm)	100×100	150×150	200×200	250×250	300×300
L_{peak} (dB)	82.9	82.7	82.4	82.3	82.2

minimum (with a PIF of 2). According to Eq.(2), the sound pressure level with a PIF of 4 was 1.2 times higher than that with a PIF of 2.

2-1-3. L_{peak} with various SEG values

The results for L_{peak} with various SEG values are listed in Table 4-3. L_{peak} decreased with increasing SEG, and there was a significant difference between SEGs values ($p < 0.017$). There was a level difference of 4.7 dB between the maximum (with a SEG of 3) and minimum (with a SEG of 11). According to Eq.(2), the sound pressure level with a SEG of 3 was 1.7 times higher than that with a SEG of 11.

2-1-4. L_{peak} with various PpF values

The results for L_{peak} with various PpF values are listed in **Table 4-4**. L_{peak} showed almost no change with decrease in PpF. There was no significant difference between any PpF values ($p>0.017$). There was a level difference of 0.2 dB between the maximum (with a PpF of 6/8) and minimum (a PpF of 7/8) with various PpF. According to Eq.(2), the sound pressure level with a PpF of 6/8 was 1.0 times higher than that with a PpF of 7/8.

2-1-5. L_{peak} with various TR values

The results for L_{peak} with various TR values are shown in **Table 4-5**. L_{peak} decreased slightly with an increase in TR. There was a significant difference, except for between TR 5000 ms and TR 5500 ms and between TR 5500 ms and TR 6000 ms ($p<0.005$). There was a level difference of 0.7 dB between the maximum (with a TR of 4030 ms) and minimum (with a TR of 6000 ms) with various TR. According to Eq.(2), the sound pressure level with a TR of 4030 ms was 1.1 times higher than that with a TR of 6000 ms.

2-1-6. L_{peak} with various MS values

The results for L_{peak} with various MS values are shown in **Table 4-6**. L_{peak} increased slightly with increasing MS. There was a significant difference, except for between MS 128×128 and MS 160×160 ($p<0.013$). There was a level difference of 0.4 dB between the maximum (with a MS of 192×192) and minimum (with MS values of 128×128 or 160×160). According to Eq.(2), the sound pressure level with a MS of 192×192 was 1.1 times higher than that with MS values of 128×128 or 160×160 .

2-1-7. L_{peak} with various ST values

The results for L_{peak} with various ST values are shown in **Table 4-7**. L_{peak} was not affected by ST. There was no significant difference between any ST values ($p>0.013$). There

was a level difference of 0.2 dB between the maximum (with a ST of 1 mm) and minimum (with ST values of 5, 7, or 10 mm). According to Eq.(2), the sound pressure level with a ST of 1 mm was 1.0 times higher than that with ST values of 5, 7, or 10 mm.

2-1-8. L_{peak} with various FOV values

The results for L_{peak} with various FOV values are shown in **Table 4-8**. L_{peak} decreased with increasing FOV. There was a significant difference, except for between FOV 200×200 mm and FOV 250×250 mm, and between FOV 250×250 mm and FOV 300×300 mm ($p<0.005$). There was a level difference of 0.7 dB between the maximum (with a FOV of 100×100 mm) and minimum (with a FOV of 300×300 mm) with various FOV. According to Eq.(2), the sound pressure level with a FOV of 100×100 mm was 1.1 times higher than that with a FOV of 300×300 mm.

2.2 Time waveform analysis

The time waveforms of acoustic noise measured with changes in various parameters are shown in **Fig.3-10**. In the time waveform, the horizontal axis represents time (ms), and the vertical axis represents sound pressure (dB). Wada et al.¹⁰⁾ reported that the amplitude of the vertical axis of the time waveform increases as the acoustic noise increases. The results of this study showed that the amplitude of the time waveform decreased with increase in ES, FOV, and SEG, and slightly decreased with decreases in PIF and MS. The amplitude of the time waveform showed little change with any of the other parameters.

Discussion

Acoustic noise in MRI, especially in DWI using single-shot echo planar imaging, is very loud, and decreasing this noise is important for decreasing discomfort and anxiety during routine clinical examinations and preventing

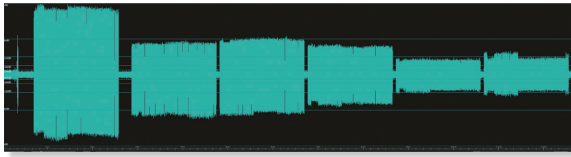


Fig.3 Waveforms of qRESOLVE with various ES values (from left to right : 0.5, 0.6, 0.7, 0.78, 0.94, and 1.0 ms)



Fig.4 Waveforms of qRESOLVE with various PIF values (from left to right : 2, 3, and 4)

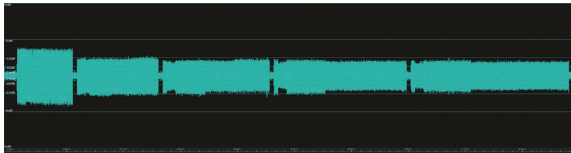


Fig.5 Waveforms of qRESOLVE with various SEG values (from left to right : 3, 5, 7, 9, and 11)

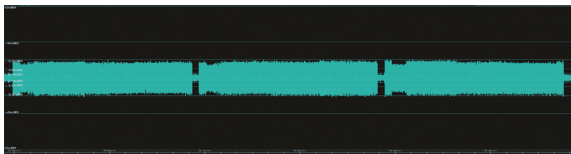


Fig.6 Waveforms of qRESOLVE with various PpF values (from left to right : Off, 7/8, and 6/8)

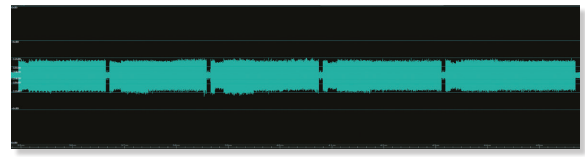


Fig.7 Waveforms of qRESOLVE with various TR values (from left to right : 4030, 4500, 5000, 5500, and 6000 ms)

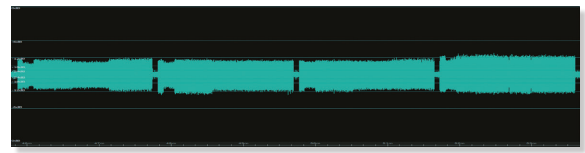


Fig.8 Waveforms of qRESOLVE with various MS values (from left to right : 128×128, 160×160, 192×192, and 226×226)

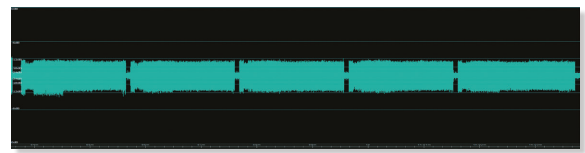


Fig.9 Waveforms of qRESOLVE with various ST values (from left to right : 1, 3, 5, 7, and 10 mm)

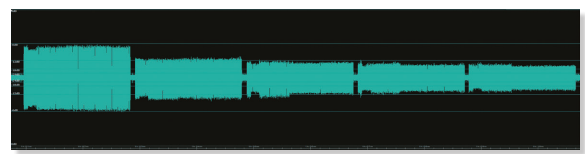


Fig.10 Waveforms of qRESOLVE with various FOV values (from left to right : 100×100, 150×150, 200×200, 250×250, and 300×300 mm)

hearing impairment. In this study, we investigated the parameters of qRESOLVE that were effective for decreasing image distortion and acoustic noise.

First, we consider image distortion. With respect to ES, the distortion rate increased with an increase in ES. With an increase in ES, the bandwidth (BW) was automatically set to narrow, resulting in an increased phase dispersion and thus an increased distortion rate. Regarding the PIF, the distortion rate decreased with an increase in the PIF. When the reading time was shortened in the phase direction, the BW was automatically set to a wide range, resulting in suppressed dephasing and thus a decreased distortion rate.

Concerning the SEG, with an increase in the

SEG, the segment width decreased to divide k-space, thus decreasing the readout time. As a result, it is expected to be effective in suppressing dephasing and decreasing image distortion. However, there was no significant difference in the distortion rate between SEGs. With an increase in SEG, the reading time of each SEG decreased, but the BW was automatically set to a narrow range; thus, the distortion rate was not change. With respect to the PpF, the distortion rate decreased with an increase in PpF. Blurring was suppressed and the distortion rate decreased with an increase in the data filling of k-space, although the BW and echo time (TE) did not change with an increase in PpF. Regarding the TR, the distortion rate did not change with an increase

in TR. The BW and TE did not change with increasing TR. Concerning MS, the distortion rate decreased with an increase in MS. The BW automatically narrowed with an increase in MS, but the magnetic field deflection in the voxel decreased, resulting in a decreased distortion rate¹¹⁾. With respect to ST, the distortion rate increased with increasing ST. The BW did not change with the ST thickness, but the magnetic field deflection in the voxel increased, resulting in an increased distortion rate¹¹⁾. Regarding the FOV, the distortion rate increased with increasing FOV. The BW automatically narrowed with an increase in FOV, and the spatial resolution also increased. Therefore, the ES, PIF, MS, ST and FOV are effective parameters for decreasing the distortion rate. However, in routine clinical examinations, MS, ST and FOV change the spatial resolution. Thus, the MS, ST and FOV are not appropriate parameters. Furthermore, it is appropriate to set PpF to “off” to avoid image distortion resulting from blurring. Therefore, a decrease in ES and an increase in PIF are effective for decreasing image distortion.

Next, we consider acoustic noise. Concerning ES, L_{peak} decreased with an increase in ES. The BW was automatically set to narrow with an increase in ES, resulting in a decrease in the angle of the gradient field. With respect to the PIF, L_{peak} increased with an increase in the PIF. The intensity of the blip applied in the phase direction increased because of the wide interval of the collected data, resulting in an increase in the angle of gradient field. Regarding the SEG, L_{peak} decreased with an increase in SEG. The BW automatically narrowed with an increase in SEG, resulting in a decrease in the angle of the gradient field. However, the scan time increased threefold with an increase in SEG (from a SEG of 3 to a SEG of 11); thus, parameter settings with an increase in SEG should be avoided. Concerning the PpF, L_{peak} did not change

with increasing PpF. The BW and TE did not change with increasing PpF. With respect to the TR, L_{peak} decreased slightly with an increase in TR. It was assumed that the BW and TE did not change, but acoustic sound was slightly lower in the longer TR than in shorter TR because the interval between acoustic sounds was wide and less affected by reverberation. Regarding the MS, L_{peak} increased slightly with an increase in MS. The BW automatically narrowed and TE increased. Generally, with a narrow in BW, resulting in a decrease in the angle of the gradient field and the acoustic noise is small. However, because the amplitude of the gradient increased simultaneously, L_{peak} was assumed to be increase. Concerning the ST, L_{peak} did not change with the thickness of ST. The BW and TE did not change with the thickness of ST. With respect to the FOV, L_{peak} decreased slightly with an increase in the FOV. With an increase in FOV, the BW was automatically set to narrow, resulting in a decrease in the angle of the gradient field. We calculated the sound pressure level difference between the maximum and minimum values of L_{peak} with various parameters using Eq.(2). The maximum value of L_{peak} was 5.1 times higher than the minimum value in ES, 1.1 times higher for FOV, 1.7 times higher for SEG, and 1.2 times higher for PIF. This suggests that an increase in ES is the most effective way to decrease acoustic noise. Individual differences in hearing are common. A decrease in acoustic noise is considered important to prevent hearing impairment. Furthermore, time waveform analysis of acoustic noise showed that an increase in ES, FOV and SEG, and a decrease in PIF and MS, are effective for decreasing the acoustic noise. Therefore, the effective parameters for decreasing acoustic noise are ES, PIF, SEG, TR, MS, and FOV. However, in routine clinical examinations, an increase in SEG prolongs scan time and increased the possibility of artifacts caused by

body motion. Therefore, a parameter setting with an SEG of 9 or higher is not appropriate. With an increase in TR, the scan time increases and the image contrast changes, while with an increase in MS, ST, and FOV, the spatial resolution changes, so they are not appropriate parameters. Therefore, an increase in ES and SEG and a decrease in PIF are effective for decreasing acoustic noise. ES, PIF, and MS are common parameters employed for decreasing image distortion and acoustic noise. However, an increase in ES decreases acoustic noise and increases image distortion, whereas a decrease in PIF and MS decreases acoustic noise and increases image distortion. Therefore, there is a trade-off relationship in the parameter setting, and further study is required. In the future, to determine the optimal scan parameter setting for decreasing image distortion and acoustic noise, we plan to evaluate the head MRI images of healthy volunteers.

Conclusion

In qRESOLVE, a decrease in image distortion was achieved with a decrease in ES and FOV, a thin slice thickness, and an increase in PIF and MS ($p < 0.017$). Furthermore, a decrease in acoustic noise was achieved with an increase in ES, SEG, TR, and FOV and a decrease in PIF and MS ($p < 0.017$). However, in routine clinical examinations, a decrease in ES and an increase in PIF are effective for decreasing image distortion, and with an increase in ES, and an increase in SEG and a decrease in PIF are effective for decreasing acoustic noise.

Conflict of interest

The author has no conflict of interest to declare.

Funding

The author received no specific funding for this work.

Acknowledgements

I would like to thank Professor Yoko Saito for her warm guidance and encouragement.

I would like to express my sincere appreciation.

表の説明

Table 1-1	ESを変化させたときのqRESOLVEのスキャンパラメーター
Table 1-2	PIFを変化させたときのqRESOLVEのスキャンパラメーター
Table 1-3	SEGを変化させたときのqRESOLVEのスキャンパラメーター
Table 1-4	PpFを変化させたときのqRESOLVEのスキャンパラメーター
Table 1-5	MSを変化させたときのqRESOLVEのスキャンパラメーター
Table 1-6	TRを変化させたときのqRESOLVEのスキャンパラメーター
Table 1-7	FOVを変化させたときのqRESOLVEのスキャンパラメーター
Table 1-8	STを変化させたときのqRESOLVEのスキャンパラメーター
Table 2	T ₂ 強調像のスキャンパラメーター
Table 3-1	ESを変化させたときの歪み率 (%)
Table 3-2	PIFを変化させたときの歪み率 (%)
Table 3-3	SEGを変化させたときの歪み率 (%)
Table 3-4	PpFを変化させたときの歪み率 (%)
Table 3-5	TRを変化させたときの歪み率 (%)
Table 3-6	MSを変化させたときの歪み率 (%)
Table 3-7	STを変化させたときの歪み率 (%)
Table 3-8	FOVを変化させたときの歪み率 (%)
Table 4-1	ESを変化させたときのピーク音圧レベル (dB)
Table 4-2	PIFを変化させたときのピーク音圧レベル (dB)
Table 4-3	SEGを変化させたときのピーク音圧レベル (dB)
Table 4-4	PpFを変化させたときのピーク音圧レベル (dB)
Table 4-5	TRを変化させたときのピーク音圧レベル (dB)
Table 4-6	MSを変化させたときのピーク音圧レベル (dB)
Table 4-7	STを変化させたときのピーク音圧レベル (dB)
Table 4-8	FOVを変化させたときのピーク音圧レベル (dB)

図の説明

- Fig.1 スリット幅測定方法
スリット両端に直行する直線を引き、 T_2 強調像のスリット幅 W_t 、qRESOLVEのスリット幅 W_q を計測した。
- Fig.2 撮像音および時間波形測定位置
撮像音および時間波形測定位置は、高さが1.3 m(床からガントリー中心部までの距離)、距離がガントリー中心部から約4.5 mで5ガウスライン(グレー線)の外側の黒丸の部分である。
- Fig.3 ESを変化させたときの撮像音の時間波形
ESを変化させたときのqRESOLVEの撮像音の時間波形である(グラフ左からESが0.5, 0.6, 0.7, 0.78, 0.94, 1.0 msec)。
- Fig.4 PIFを変化させたときの撮像音の時間波形
PIFを変化させたときのqRESOLVEの撮像音の時間波形である(グラフ左からPIFが2, 3, 4)。
- Fig.5 SEGを変化させたときの撮像音の時間波形
SEGを変化させたときのqRESOLVEの撮像音の時間波形である(グラフ左からSEGが3, 5, 7, 9, 11)。
- Fig.6 PpFを変化させたときの撮像音の時間波形
PpFを変化させたときのqRESOLVEの撮像音の時間波形である(グラフ左からPpFがOff, 7/8, 6/8)。
- Fig.7 TRを変化させたときの撮像音の時間波形
TRを変化させたときのqRESOLVEの撮像音の時間波形である(グラフ左からTRが4030, 4500, 5000, 5500, 6000 msec)。
- Fig.8 MSを変化させたときの撮像音の時間波形
MSを変化させたときのqRESOLVEの撮像音の時間波形である(グラフ左からMSが128×128, 160×160, 192×192, 226×226)。
- Fig.9 STを変化させたときの撮像音の時間波形
STを変化させたときのqRESOLVEの撮像音の時間波形である(グラフ左からSTが1, 3, 5, 7, 10 mm)。
- Fig.10 FOVを変化させたときの撮像音の時間波形
FOVを変化させたときのqRESOLVEの撮像音の時間波形である(グラフ左からFOVが100×100, 150×150, 200×200, 250×250, 300×300 mm)。

参考文献

- 1) M. E. Bastin: Correction of eddy current-induced artefacts in diffusion tensor imaging using iterative cross-correlation. *Magn Reson Imaging*, 17(7), 1011-1024, 1999.
- 2) D. A. Porter, et al.: High resolution diffusion-weighted imaging using readout-segmented echo-planar imaging, parallel imaging and a two-dimensional navigator-based reacquisition. *Magn Reson Med*, 62(2), 468-475, 2009.
- 3) O. Martin, et al.: Acoustic-noise-optimized diffusion-weighted imaging. *Magn Reson Mater Phy*, 28, 511-521, 2015.
- 4) R. Julie, et al.: Quiet Diffusion-Weighted Head Scanning: Initial Clinical Evaluation in Ischemic Stroke Patients at 1.5T. *J. MAGN. RESON. IMAGING*, 44(5), 1238-1243, 2016.
- 5) M. A. Griswold, et al.: Generalized Autocalibrating Partially Parallel Acquisitions (GRAPPA). *Magn Reson Med*, 47(6), 1202-1210, 2002.
- 6) Y. Kaneko, et al.: Using the area mismatch with SE images to evaluate the distortion of EPI. *Japan Journal of Magnetic Resonance in Medicine*, 36(3), 98-105, 2016.
- 7) M. Kajisako, et al.: Experience with Siemens' RESOLVE (readout segmented EPI DWI). *Rad Fun*, 10(5), 11-14, 2012.
- 8) K. Kuno, et al.: Acoustic noise measurement and evaluation/dB and LAeq. Tokyo, Japan, Gihoudo publishing co., 28-31, 2006.
- 9) Y. Kanda : Investigation of the freely available easy-to-use software "EZR"(Easy R)for medical statistics. *Bone Marrow Transplantation*, 48, 452-458, 2013.
- 10) T. Wada, et al.: Analysis of the acoustic sound in MRI. *Oto-Rhino-Laryngology*, Tokyo, 42(1), 131-135, 1999.
- 11) T. Aoki, et al.: 3-Tesla MR Imaging of the pelvis. *Japanisch-Deutsche Medizinische Berichte*, 52(1), 47-52, 2007.